

A Simple Method to Detect Atrial Fibrillation Using RR Intervals

Jie Lian, PhD^{a,*}, Lian Wang, MS^b, and Dirk Muessig, PhD^a

Implantable loop recorders have been developed for long-term monitoring of cardiac arrhythmia, but their accuracy for atrial fibrillation (AF) detection is unsatisfactory. We sought to develop and evaluate a simple method for detecting AF using RR intervals. The new AF detection algorithm is based on a map that plots RR intervals versus change of RR intervals (RdR). The map is divided by a grid with 25-ms resolution in 2 axes and nonempty cells are counted to classify AF and non-AF episodes. We evaluated the performance of the method using 4 PhysioNet databases: MIT-BIH AF database, MIT-BIH arrhythmia database, MIT-BIH normal sinus rhythm (NSR) database, and NSR RR interval database (total 145 patients, 1,826 hours NSR, 96 hours AF, and 11 hours other rhythms). Each record is divided into consecutive windows containing 32, 64, or 128 RR intervals. AF detection is performed for each window and classification results are compared to annotations. A window is labeled true AF if $>1/2$ of cycles in the window are annotated as AF or non-AF otherwise. The RdR map shows signature patterns corresponding to various heart rhythms. Optimal nonempty cell cut-off threshold for AF detection was determined by receiver operating characteristic curve analysis, which yields excellent sensitivity and specificity for window sizes 32 (94.4% and 92.6%, respectively), 64 (95.8% and 94.3%), and 128 (95.9% and 95.4%). In conclusion, a single metric derived from the RdR map can achieve robust AF detection within as few as 32 heart beats. © 2011 Elsevier Inc. All rights reserved. (Am J Cardiol 2011;107:1494–1497)

Many atrial fibrillation (AF) episodes are asymptomatic^{1,2}; thus reliable AF detection is needed to gauge the success of antiarrhythmic therapy. Many algorithms have been developed to detect AF by assessing regularity of RR intervals.^{3–12} However, these algorithms are limited by their computational complexity or unsatisfactory performance. In the present report, we present a simple yet robust method for AF detection using RR intervals.

Methods

The new AF detection algorithm is based on a map that shows the scatterplot of RR intervals versus change of RR intervals (dRRs; RdR map). Denote RR_i , a series of RR intervals, where RR_i represents the i -th RR interval. Further denote dRR_i , a series of differences between 2 adjacent RR intervals, i.e., $dRR_i = RR_i - RR_{i-1}$. The RdR map is constructed by plotting the RR interval series in 1 axis (e.g., x) against the dRR series in another axis (e.g., y). Number of data points in the RdR map equals the length of the dRR series, and each data point represents 1 pair of RR interval and corresponding dRR interval.

Different from the conventional Lorenz plot, which is based on RR intervals^{3,11} or dRR intervals,⁴ the RdR map embeds RR intervals and dRR intervals in the same plot. As a result, heart rate (RR interval) and heart rate change (dRR) information are readily available for use in cardiac rhythm classification.

As would be appreciated from the following examples (Figure 1), different heart rhythms show distinctive spatial distribution patterns in their RdR maps. In particular, AF rhythm is characterized by random data points scattered in a large area of the RdR map, reflecting irregularity in RR intervals and change of RR intervals. To quantify the sparseness of data points, the RdR map is divided by a 2-dimensional grid with 25-ms resolution in the 2 axes, and nonempty cells (NECs; i.e., contain ≥ 1 data point) are counted. For an episode of cardiac cycles (number of data points set to 32, 64, and 128 in this study), detection of AF rhythm is made if NEC exceeds a predefined threshold. Otherwise, non-AF classification is made.

Performance of the new AF detection algorithm was evaluated using 4 annotated PhysioNet databases¹³ (MIT-BIH AF database, MIT-BIH arrhythmia database, MIT-BIH normal sinus rhythm [NSR] database, and NSR RR interval database; Table 1). All together, these databases include 144 patients and provide RR interval data that include 1,826 hours NSR, 96 hours AF rhythm, and 11 hours other rhythms.

Each patient's record is divided into consecutive (non-overlapping) windows containing 32, 64, or 128 RR intervals. For reference, a window is labeled a true AF episode if $>1/2$ of cycles in the window are annotated as AF; otherwise the episode is non-AF. For each window, AF detection is performed and the classification result (AF or non-AF) is compared to the reference (labeled based on

^aMicro Systems Engineering, Inc., Lake Oswego, Oregon; ^bProvidence Heart and Vascular Institute, Portland, Oregon. Manuscript received December 17, 2010; revised manuscript received and accepted January 18, 2011.

This work is fully supported by Biotronik SE and Co. KG, Berlin, Germany.

This work was presented in part at the 31st Annual Scientific Sessions of the Heart Rhythm Society, Denver, Colorado, May 12 to 15, 2010, and published in abstract form (*Heart Rhythm* 2010;7(suppl):S387, PO6–16).

*Corresponding author: Tel: 503-744-8634; fax: 503-635-9610.

E-mail address: jie.lian@biotronic.com (J. Lian).

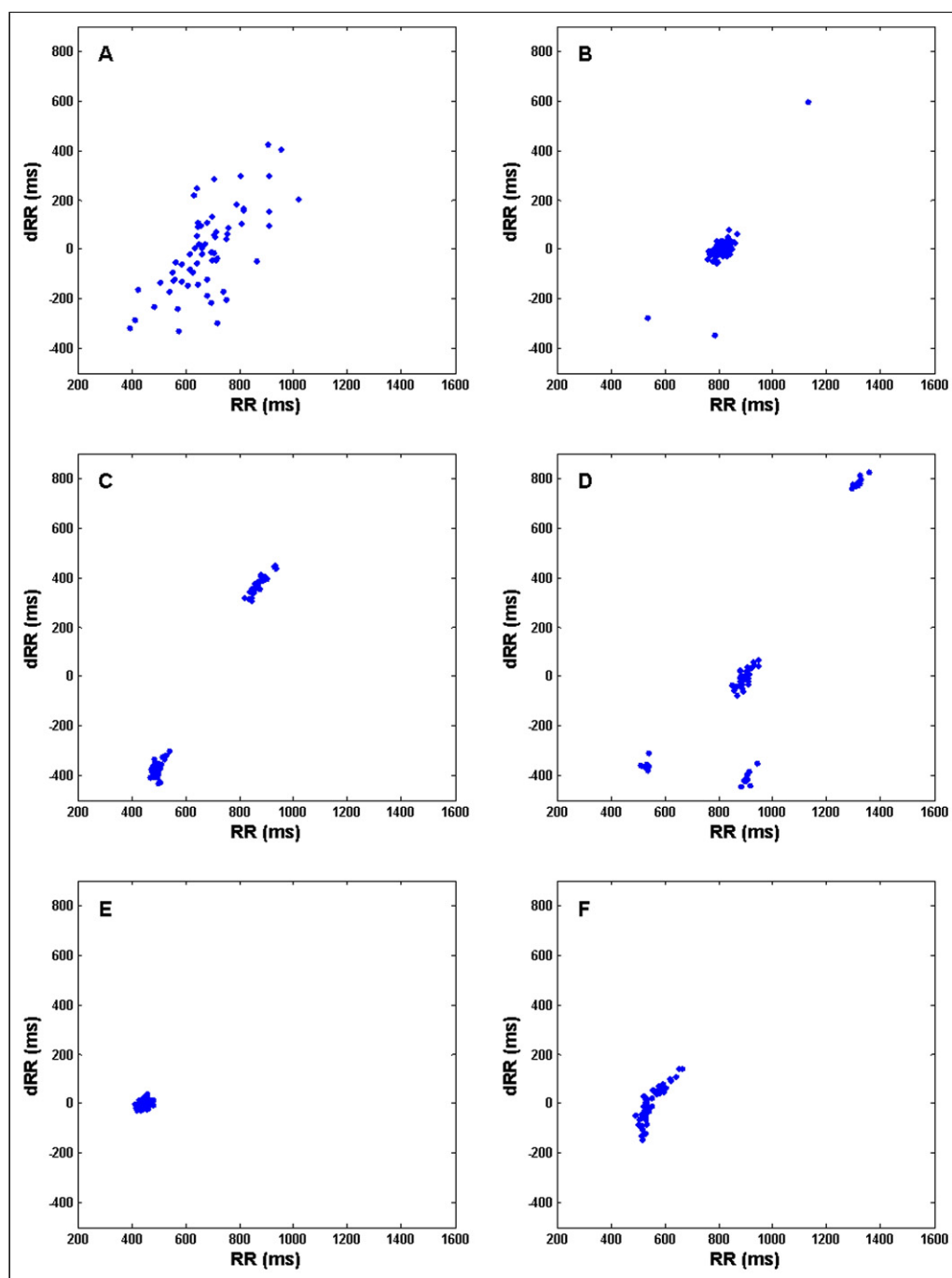


Figure 1. Representative examples of maps plotting RR intervals versus change of RR intervals corresponding to (A) atrial fibrillation rhythm, (B) normal sinus rhythm with 1 premature ventricular complex, (C) persistent ventricular bigeminy, (D) mixed sinus rhythm and ventricular trigeminy, (E) typical atrial flutter, and (F) ventricular tachycardia. The window size is set to 64 in these examples.

Table 1
Databases used in the study

Database	Number of Records	Duration of NSR Rhythm (hours)	Duration of AF Rhythm (hours)	Duration of Other Rhythms (hours)
MIT-BIH normal sinus rhythm database	18	384	0	0
Normal sinus rhythm RR interval database	54	1276	0	0
MIT-BIH atrial fibrillation database	25	149.1	93.3	6.6
MIT-BIH arrhythmia database	48	17.3	2.2	4.5
Combined databases	145	1826.4	95.5	11.1

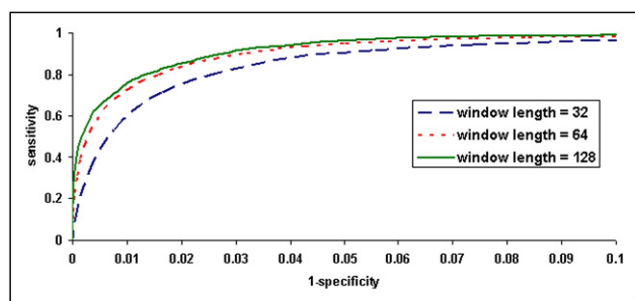


Figure 2. Receiver operating characteristic curves for atrial fibrillation detection corresponding to 3 different window sizes (32, 64, and 128) by changing the nonempty cell cut-off threshold.

annotations) to determine if it is true positive, false positive, true negative, or false negative. Sensitivity and specificity of AF detection are then calculated for each database and the combined databases. For each window size, receiver operating characteristic curve is obtained by changing the NEC threshold and area under the receiver operating characteristic curve is calculated. Optimal NEC cut-off threshold for AF detection is determined by searching for the shortest distance to the upper left corner.¹⁴

Results

Figure 1 shows representative examples of RdR maps corresponding to various heart rhythms. In general, distribution of data points is oriented from the lower left to the upper right of the RdR map because longer RR intervals tend to have positive dRR intervals, whereas shorter RR intervals are often associated with negative dRR intervals.

Clearly different cardiac rhythms show distinctive patterns on an RdR map. AF rhythm is characterized by scattered data points distributed in a large area (Figure 1), reflecting the irregularity of heart rate and change of heart rate. In contrast, other rhythms show ≥ 1 cluster in their RdR maps (Figure 1), implying the presence of a certain degree of rate and/or rhythm regularity. Note that a single premature ventricular complex during NSR generated 3 isolated data points because of the short premature ventricular complex coupling interval, long pause after the premature ventricular complex, and the following return to normal RR interval (Figure 1). Similarly, 3 additional clusters are generated in ventricular trigeminy rhythm, which has multiple “short–long–normal” cycles (Figure 1). In contrast, persistent ventricular bigeminy has a signature pattern of dual clusters because of the repetitive short–long sequence (Figure 1).

Calculated from the combined databases, Figure 2 shows AF detection receiver operating characteristic curves corresponding to 3 different window sizes (32, 64, and 128) by changing the NEC cut-off threshold. Areas under receiver operating characteristic curves are 0.978, 0.986, and 0.989 for the 3 window sizes, respectively. As expected, larger window size yields more robust AF detection. Optimal NEC cut-off thresholds were 23, 40, and 65 corresponding to window sizes 32, 64, and 128, respectively. Using optimal NEC cut-off threshold for each window size, Table 2 presents AF detection results in each dataset and combined

databases. Overall, excellent sensitivity and specificity for AF detection are obtained for window sizes 32 (94.4% and 92.6%, respectively), 64 (95.8% and 94.3%), and 128 (95.9% and 95.4%).

Discussion

This study presents a novel method for AF detection based on an RdR map constructed from RR intervals. Although increasing the window could yield more robust AF detection, excellent performance ($>90\%$ in sensitivity and specificity) could be achieved when analyzing only 32 cardiac cycles. Therefore, this method is well suited for real-time AF detection.

The hallmark of AF is an irregularly irregular ventricular rhythm. Such irregularity is often manifested in heart rate and change of heart rate, which are respectively embedded in 2 dimensions of the RdR map. In contrast, conventional AF detection methods usually measure only irregularity in RR intervals^{3,5,11} or dRR intervals^{4,5,8}; thus important rhythm information (on heart rate change or heart rate) may be excluded. Therefore, although technically the RdR map may appear to be only a minor deviation from the conventional Lorenz plot,^{3,4,11} conceptually the RdR map represents a fundamental departure from the Lorenz plot approach because it embeds 2 (instead of 1) independent sources of heart rhythm information (heart rate and change of heart rate) into a single graph.

Direct comparison with other AF detection methods is hindered by nonuniform usage of test databases and/or performance metrics. Similar to Shouldice et al,⁶ we evaluated our algorithm in 4 large public databases, whereas most other studies used smaller/partial database or proprietary data.^{3–5,7–10,12,15} In this study, we used the standard definition of episode sensitivity and specificity, which are the most meaningful clinical measurements of true-positive rate and true-negative rate. The commonly used positive predictive value,^{4–6,8,12} however, is affected by AF prevalence. Another unique advantage of the present method is its simplicity. Classification of AF and non-AF is based on a single metric NEC, which is a simple count of NECs on the RdR map. All other methods require evaluation of multiple metrics and/or more complex calculations usually involving floating point operations that are particularly challenging for implementation in battery-powered implantable devices.

The present AF detection method is particularly suitable for implementation in implantable loop recorders because of its high efficiency and accuracy, thus offering an attractive device feature for long-term cardiac rhythm monitoring and diagnosis, which may be used to assess the efficacy of antiarrhythmic therapy and guide anticoagulation management in patients with AF.¹⁵ Furthermore, the intuitive RdR map offers a new way of analyzing cardiac rhythms. Although we have explored using only 1 metric for AF detection, the combination of multiple metrics may facilitate discrimination of various cardiac arrhythmias because their distinctive RdR patterns (Figure 1).

This study is limited mainly by the retrospective analysis of available databases that may not be representative of clinical data. Independent performance evaluation in a prospective dataset is highly desired. We also did not evaluate

Table 2

Atrial fibrillation detection results using optimal nonempty cell cut-off thresholds

Database	Window Size 32		Window Size 64		Window Size 128	
	Sensitivity	Specificity	Sensitivity	Specificity	Sensitivity	Specificity
MIT-BIH normal sinus rhythm database	NA*	84.1%	NA*	87.4%	NA*	90.0%
Normal sinus rhythm RR interval database	NA*	95.1%	NA*	96.4%	NA*	97.2%
MIT-BIH atrial fibrillation database	94.3%	95.1%	95.7%	96.0%	95.8%	96.4%
MIT-BIH arrhythmia database	98.1%	77.0%	97.7%	78.2%	98.9%	78.8%
Combined databases	94.4%	92.6%	95.8%	94.3%	95.9%	95.4%

* Calculation of sensitivity is not applicable for the MIT-BIH normal sinus rhythm and normal sinus rhythm RR interval databases because of the absence of a true atrial fibrillation episode.

NA = not applicable.

effects of RR interval artifacts frequently seen in clinical practice, e.g., because of T-wave oversensing, R-wave undersensing, noise interference, etc. In addition, like all other RR interval-based algorithms, the present method may fail to detect AF with relatively regular rhythm and produce a false alarm for non-AF rhythm with a certain degree of rhythm irregularity.

Supplementary data

Supplementary data associated with this article can be found, in the online version, at [doi:10.1016/j.amjcard.2011.01.028](https://doi.org/10.1016/j.amjcard.2011.01.028).

- Orlov MV, Ghali JK, Araghi-Niknam M, Sherfese L, Sahr D, Hettrick DA. Asymptomatic atrial fibrillation in pacemaker recipients: incidence, progression, and determinants based on the atrial high rate trial. *Pacing Clin Electrophysiol* 2007;30:404–411.
- Verma A, Minor S, Kilicaslan F, Patel D, Hao S, Beheiry S, Lakireddy D, Elayi SC, Cummings J, Martin DO, Burkhardt JD, Schweikert RA, Saliba W, Tchou PJ, Natale A. Incidence of atrial arrhythmias detected by permanent pacemakers (PPM) post-pulmonary vein antrum isolation (PVAI) for atrial fibrillation (AF): correlation with symptomatic recurrence. *J Cardiovasc Electrophysiol* 2007;18:601–606.
- Park J, Lee S, Jeon M. Atrial fibrillation detection by heart rate variability in Poincare plot. *Biomed Eng Online* 2009;8:38.
- Sarkar S, Ritscher D, Mehra R. A detector for a chronic implantable atrial tachyarrhythmia monitor. *IEEE Trans Biomed Eng* 2008;55:1219–1224.
- Ghodrat A, Murray B, Marinello S. RR interval analysis for detection of atrial fibrillation in ECG monitors. *Conf Proc IEEE Eng Med Biol Soc* 2008;2008:601–604.
- Shouldice RB, Heneghan C, de Chazal P. Automated detection of paroxysmal atrial fibrillation from inter-heartbeat intervals. *Conf Proc IEEE Eng Med Biol Soc* 2007;2007:686–689.
- Kikillus N, Hammer G, Wieland S, Bolz A. Algorithm for identifying patients with paroxysmal atrial fibrillation without appearance on the ECG. *Conf Proc IEEE Eng Med Biol Soc* 2007;2007:275–278.
- Petrucchi E, Balian V, Filippini G, Mainardi LT. Atrial fibrillation detection algorithms for very long term ECG monitoring. *Comput Cardiol* 2005;32:623–626.
- Duverney D, Gaspoz JM, Pichot V, Roche F, Brion R, Antoniadis A, Barthelemy JC. High accuracy of automatic detection of atrial fibrillation using wavelet transform of heart rate intervals. *Pacing Clin Electrophysiol* 2002;25:457–462.
- Tateno K, Glass L. Automatic detection of atrial fibrillation using the coefficient of variation and density histograms of RR and deltaRR intervals. *Med Biol Eng Comput* 2001;39:664–671.
- Anan T, Sunagawa K, Araki H, Nakamura M. Arrhythmia analysis by successive RR plotting. *J Electrocardiol* 1990;23:243–248.
- Moody GB, Mark RG. A new method for detecting atrial fibrillation using R-R intervals. *Comput Cardiol* 1983;10:227–230.
- Goldberger AL, Amaral LA, Glass L, Hausdorff JM, Ivanov PC, Mark RG, Mietus JE, Moody GB, Peng CK, Stanley HE. PhysioBank, PhysioToolkit, and PhysioNet: components of a new research resource for complex physiologic signals. *Circulation* 2000;101(suppl):E215–E220.
- Sun XG, Hansen JE, Beshai JF, Wasserman K. Oscillatory breathing and exercise gas exchange abnormalities prognosticate early mortality and morbidity in heart failure. *J Am Coll Cardiol* 2010;55:1814–1823.
- Hindricks G, Pokushalov E, Urban L, Taborsky M, Kuck KH, Lebedev D, Rieger G, Purerfellner H. Performance of a new leadless implantable cardiac monitor in detecting and quantifying atrial fibrillation: results of the XPECT trial. *Circ Arrhythmia Electrophysiol* 2010;3:141–147.